

# Hammett Studies on Alkene Extrusion from Rhenium(V) Diolates and an MO Description of Metal Alkoxide–Alkyl Metal Oxo Interconversion

Kevin P. Gable\*<sup>1</sup> and Jerrick J. J. Juliette

Contribution from the Department of Chemistry, Oregon State University, Corvallis, Oregon 97331-4003

Received July 28, 1995<sup>⊗</sup>

**Abstract:** Rates of cycloreversion of phenyl-substituted diolates of the type Cp\*Re(O)(diolate), where diolate = phenylethane-1,2-diolate, exhibited a linear relationship with Hammett  $\sigma^-$  constants, with  $\rho = 0.42$ . This suggests a slight buildup of electron density but little charge development in the transition state. The better fit with  $\sigma^-$  constants suggests a resonance interaction between the phenyl ring and the breaking C–O bond. On the other hand, similar 1,2-diphenylethane-1,2-diolates showed curved Hammett behavior, with acceleration by electron-donating and electron-withdrawing groups. Such behavior offers more evidence for a nonsymmetric transition state and stepwise cleavage of the C–O bonds. Molecular orbital calculations suggest a rationale for bonding changes in these systems.

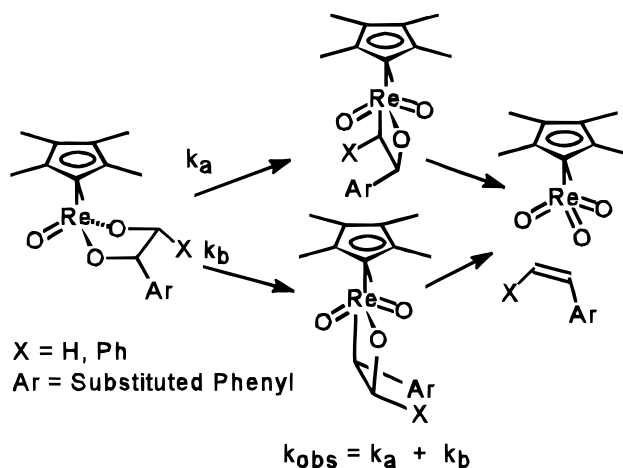
## Introduction

We have previously examined several aspects of diolate cycloreversions in the system Cp\*Re(O)(diolate).<sup>2</sup> The primary goal has been to understand whether bond cleavage is concerted or stepwise. Application of the principle of microscopic reversibility offers insight into whether the C–O bond-forming processes in alkene oxidations occur only at oxygen or whether participation of the metal center is involved.

Among the findings of these earlier experiments are the following: (1) The enthalpy of activation does not correlate (and is almost invariant) with strain in the newly formed double bond.<sup>2a</sup> This implies there is no  $sp^2$  character in the reacting carbon in the transition state. (2) There is a substantial secondary deuterium kinetic isotope effect,<sup>2a</sup> implying significant cleavage of at least one C–O bond in the transition state. (3) A correlation exists between reactivity and average diolate structure in which a staggered conformation leads to faster reaction rates than an eclipsed conformation.<sup>2b</sup> This suggests orientation of one C–O bond relative to the metal's coordination sphere is more important than its alignment with the second C–O bond. (4) The reaction is stereospecific, and no rearrangements (e.g., in 2-norbornyl systems) are observed.<sup>2a</sup> These studies have offered evidence that the formation of alkenes and Cp\*ReO<sub>3</sub> is not a concerted process, nor does it involve radical or carbocation intermediates. However, we find only limited and circumstantial evidence for the structure of the intermediate whose presence is inferred from nonconcertedness. The ability of Hammett studies to gain insight into the nature of the transition state in mechanistic studies led us to examine such behavior for these rhenium(V) diolates.

Linear free energy studies have long offered mechanistic chemists useful insight into the relationship between structure and energetics.<sup>3</sup> In many cases they have provided important evidence concerning the nature of transition states for chemical

## Scheme 1



transformations. Where the electronic changes induced at a particular site in a known process closely parallel those induced at a similar site in an uncharacterized process, a linear relationship among free energy measurements (normally  $\log K_{\text{eq}}$  for equilibrium measurements, and  $\log k_{\text{obs}}$  for kinetic measurements) can be seen. The slope of this line represents a quantitative measurement of whether these electronic changes are more or less important than in the reference, and the sign of the slope normally reflects whether electron density at the reactive site is increasing or decreasing on going to the transition state. On the other hand, a process for which a change in the electronic nature of the substituent induces a change in mechanism, or a change in global transition state in a multistep mechanism, often exhibits a curved plot.<sup>4</sup>

An important hypothesis arising from our earlier studies on rhenium diolate fragmentations has been that the rate-determining step is migration of carbon from oxygen to rhenium to form

<sup>⊗</sup> Abstract published in *Advance ACS Abstracts*, March 1, 1996.

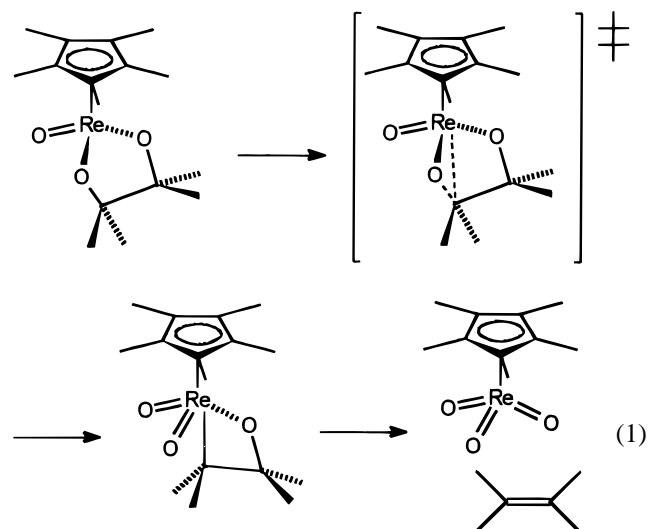
(1) Internet: gablek@ccmail.orst.edu

(2) (a) Gable, K. P.; Phan, T. N. *J. Am. Chem. Soc.* **1994**, *116*, 833–839. (b) Gable, K. P.; Juliette, J. J. *J. Am. Chem. Soc.* **1995**, *117*, 955–962.

(3) (a) Johnson, C. D. *The Hammett Equation*. Cambridge University Press: Cambridge, 1980. (b) Hansch, C.; Leo, A.; Taft, R. W. *Chem. Rev.* **1991**, *91*, 165–195. (c) Ehrenson, S. *Progr. Phys. Org. Chem.* **1964**, *2*, 195–251.

(4) Carey, F. A.; Sundberg, R. J. *Advanced Organic Chemistry*, 3rd Ed., Part A; Plenum: New York, 1990; pp 207–208.

a metallaoxetane (eq 1).<sup>5</sup> Since no intermediate accumulates, it must then (if it exists) fragment rapidly to Cp\*ReO<sub>3</sub> and alkene. A necessary element of this mechanism is the loss of



symmetry: the two diolate carbons (ignoring substituents) are equivalent in the diolate, yet distinct in the intermediate and transition state. Careful electronic control of substituents on these carbons should offer the opportunity to demonstrate this loss of symmetry (Scheme 1). Altering the electronic nature of the aryl group should alter the competition between  $k_a$  and  $k_b$ . Since each of these processes will have a different dependence on the aryl substituent (Hammett  $\rho$ ), a curved plot of  $\log(k_{\text{obs}})$  vs substituent parameter should be observed.

## Results and Discussion

**1. Phenylethanediolates.** A series of substituted phenylethanediolates were prepared via a known route.<sup>6</sup> The starting diolates were all predominantly in the anti-geometry, judging from comparison of <sup>1</sup>H NMR shifts to those of other similar compounds.<sup>2a</sup> In most instances, both syn and anti isomers are present; the anti was followed for kinetic studies although both reacted at comparable rates for each compound. As in our earlier studies, disappearance of starting material was monitored by NMR; the Cp\* signals at 1.65–1.80 ppm normally offered the optimum signal-to-noise values, although other signals for the diolate portion could be used to double-check relative concentrations. Figure 1 shows the plot of these rate constants<sup>7</sup> (C<sub>6</sub>D<sub>6</sub>, reaction temperature 40.1 °C) as a function of Hammett  $\sigma^-$  (values taken from ref 3b).

We do not observe the anticipated curvature, but close examination of reaction energetics reveals that the slowest substituent still proceeds at a rate faster than that of the ethanediolate,<sup>2a</sup> the prototype for CH<sub>2</sub> migration. For ethylene extrusion, the extrapolated mechanistic  $k_a$  (313 K) =  $3.2 \times 10^{-8} \text{ s}^{-1}$ , ( $\Delta G^\ddagger = 29.1 \text{ kcal/mol}$ ) after statistical correction for symmetry. At this same temperature, the slowest styrene extrusion, *p*-methoxy, proceeds at an observed rate  $k = 5.2 \pm 0.3 \times 10^{-6} \text{ s}^{-1}$ , with  $\Delta G^\ddagger = 25.9 \text{ kcal/mol}$ . Therefore, one may conclude that if the mechanism in eq 1 is operating, then we see only migration of the phenyl-bearing carbon.

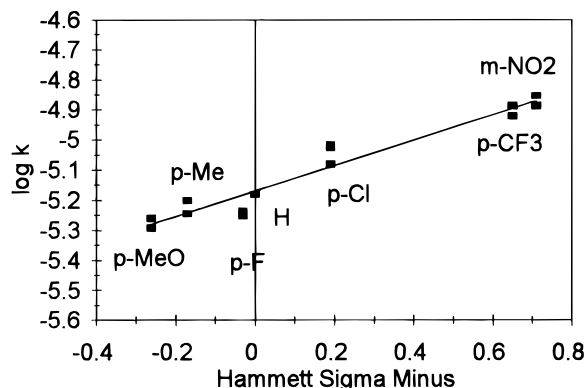
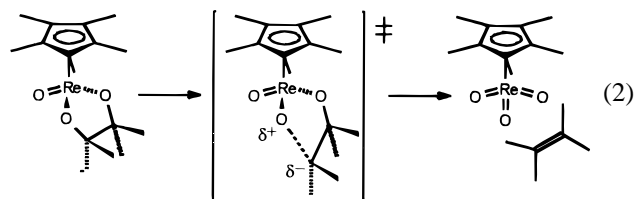


**Figure 1.** Hammett plot for extrusion of substituted styrenes. Based on  $\sigma^-, \rho = 0.42$ ,  $r^2 = 0.94$ . Each rate was measured in triplicate.

**Table 1.** Solvent Effects on Extrusion of *p*-Chlorostyrene at 50.1 °C

solvent	$k_{\text{obs}}, 10^{-5} \text{ s}^{-1}$	$\epsilon^{10}$
C <sub>6</sub> D <sub>6</sub>	$3.2 \pm 0.3$	2.28
THF-d <sub>8</sub>	$3.0 \pm 0.3$	7.32
CD <sub>3</sub> CN	$3.0 \pm 0.3$	36.2
acetone-d <sub>6</sub>	$2.8 \pm 0.3$	27

Other useful mechanistic information is evident in Figure 1. The slope of this plot,  $r = +0.42$ , suggests an increase in electronic density at the benzylic carbon. One rationale is that this proceeds through an “asynchronous concerted” transition state<sup>8</sup> eq (2). There are problems with this proposal. The



intermediate would have to retain a significant O–C interaction to prevent loss of stereochemistry expected from any free carbanion. If one assumes this interaction at the transition state, it is questionable whether the changes in normal modes of the C–H bonds would be large enough to produce the observed secondary kinetic isotope effect. For example, in the E1cb elimination from *p*-NO<sub>2</sub>C<sub>6</sub>H<sub>4</sub>CH(T)CH<sub>2</sub>NMe<sub>3</sub><sup>+</sup> the measured secondary  $k_{\text{H}}/k_{\text{T}} = 1.15$ .<sup>9</sup> This corresponds to a deuterium KIE of 1.10, which is similar to our measured<sup>2a</sup> per-deuterium KIE of 1.12 (assuming cleavage of a single C–O bond at the transition state). Further, if the bond stretch occurs to a sufficient extent to produce such a KIE, one would expect significant polarization of the molecule as a whole and a large solvent effect. Table 1 demonstrates that this effect is negligible, consistent with the minimal charge buildup expressed by  $\rho < 1$ . The combination of a low  $\rho$  value and negligible solvent effect suggests that electronic reorganization is occurring within the coordination sphere of the metal, in that changes in individual bond polarities cancel each other leading to little net change in the polarity of the molecule.

Finally, this hypothesis predicts that extrusion of styrene and stilbene will occur at approximately the same rate and that

(5) (a) Sharpless, K. B.; Teranishi, A. Y.; Bäckvall, J.-E. *J. Am. Chem. Soc.* **1977**, *99*, 3120–3128. (b) Hentges, S. G.; Sharpless, K. B. *J. Am. Chem. Soc.* **1980**, *102*, 4263–4265. (c) Jørgensen, K. A.; Schiott, B. A. *Chem Rev.* **1990**, *90*, 1483–1506.

(6) Gable, K. P. *Organometallics* **1994**, *13*, 2486–2488.

(7) See Tables 3–6 in Experimental Section.

(8) Brookhart, M.; Tucker, J. R.; Husk, G. R. *J. Am. Chem. Soc.* **1983**, *105*, 258–264.

(9) Hodnett, E. M.; Flynn, J. J., Jr. *J. Am. Chem. Soc.* **1957**, *79*, 2300–2302.

(10) Gordon, A. J.; Ford, R. A. *The Chemist's Companion*; Wiley-Interscience: New York, 1972; pp 4–13.

**Table 2.** Activation Parameters for Alkene Extrusion from Phenyl-Substituted Diolates

product	$\Delta H^\ddagger$ , kcal/mol	$\Delta S^\ddagger$ , cal/(mol-K)	rate, 323 K, s <sup>-1</sup>	ref
CH <sub>2</sub> =CH <sub>2</sub>	28.0 ± 0.1	-2.1 ± 1.2	2.6 × 10 <sup>-7</sup>	2a
PhCH <sub>2</sub> =CH <sub>2</sub>	26.1 ± 0.1	0.6 ± 0.1	2.0 × 10 <sup>-5</sup>	2b
(Z)-PhCH=CHPh	27.9 ± 0.2	2.8 ± 0.8	3.6 × 10 <sup>-6</sup>	this work
(E)-PhCH=CHPh	24.2 ± 0.7	-0.8 ± 4.3	1.9 × 10 <sup>-4</sup>	this work

differences may be attributed only to a steric effect based on whether the phenyl group on the reacting carbon is syn or anti to the Cp\* ring. This is clearly not true (see Table 2 and discussion below).

If the reaction were concerted, but with a transition state having one strong and one weak C–O bond, then one would expect to see essentially the same rate (or at least  $\Delta H^\ddagger$ ) for styrene and stilbene extrusions. This is true regardless of whether one posits a “carbanion-like” or a “radical-like” transition state. Only the syn/anti position of the phenyl group should matter due to potential steric interactions with the Cp\* ring. Estimates of such steric interactions based on molecular mechanics calculations (see below) indicate the closest H<sub>ph</sub>–H<sub>Cp\*</sub> distance in the *trans*-stilbene diolate is approximately 2.3 Å, too far apart to lead (by itself) to the almost 4 kcal/mol acceleration seen for this isomer.

Alternatively, if the mechanism in Scheme 1 operates, one might question whether a migration of carbon (with its electrons) ought to show a positive  $\rho$  value, since in the transition state, the filled C–O bond must mix with an empty metal orbital. Certainly, many electrophilic rearrangements fit this model and show negative  $\rho$  values.<sup>11</sup> However, migrations to and from metal centers impose an additional effect not normally seen in reactions of second-row main group compounds, and this is the dramatic change in polarization of the migrating bond due to electronegativity changes. Stille and Regan observed an example where this effect may predominate in the decarbonylation of benzoyl chlorides by rhodium complexes,<sup>12</sup> where  $r = +0.265$  for migration from CO to rhodium. As these authors point out, such a result can be explained by the change in electron demand when carbon moves from (electron-withdrawing) carbonyl to the (electron rich) metal. However, small changes in the structure of the migrating group may change the location of the transition state and the particular demands of the migrating group; phenylacetyl decarbonylation in the same system shows  $\rho = -0.612$ . These results point out the danger in overinterpreting the sign of  $\rho$  in reactions involving migrations; the electron demand of carbon in the transition state may shift with subtle structural modification. However, one clearly expects small  $\rho$  values, consistent with what is seen in Figure 1.

Our mechanistic proposal (eq 1) involves migration of a benzylic carbon from O to Re. Because no reactive intermediate accumulates during the reaction, this will not be an exothermic reaction<sup>13</sup> (in contrast to many organic migration reactions).

(11) (a) Thyagarajan, B. S., Ed. *Mechanisms of Molecular Migrations*; Wiley-Interscience: New York, 1971. (b) de Mayo, P., Ed. *Rearrangements in Ground and Excited States*. Academic: New York, 1980.

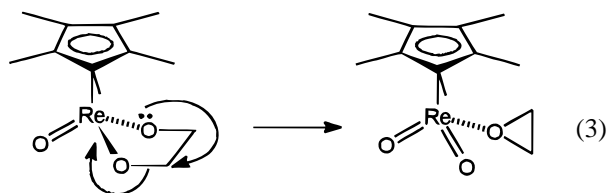
(12) Stille, J. K.; Regan, M. T. *J. Am. Chem. Soc.* **1974**, *96*, 1508–1514.

(13) Examination of the reverse process with strained alkenes also fails to reveal buildup of an intermediate, despite the approximate thermodynamic parity of diolates and alkene/Cp\*ReO<sub>3</sub> mixtures (refs 2a, 32). If the first step in diolate cycloreversion were highly exothermic ( $\Delta H^\circ < -5$  kcal/mol) we would be able to detect the intermediate in the reverse reaction for oxidation of highly strained alkenes. Actually, this reveals that the reaction is not exothermic; however, for a unimolecular rearrangement,  $\Delta S^\circ \approx 0$  and so extrapolation to saying that  $\Delta H^\circ \geq -5$  kcal/mol for the first step is justified. We thank a referee for pointing out the distinction.

Therefore, the transition state is more productlike than reactantlike. This is precisely the kind of situation where net changes in bonding will be most significantly expressed in the transition state. The different electronegativities of the two atoms (O = 3.44, Re = 1.9, C (sp<sup>3</sup>) = 2.48)<sup>14</sup> will result in a change in polarization (C<sup>δ+</sup>–O<sup>δ-</sup> to C<sup>δ-</sup>–Re<sup>δ+</sup>); stabilization of the intermediate by electron-withdrawing groups on carbon will lower the transition state energy according to the Hammond postulate.<sup>15</sup>

The observed improvement in correlation with  $\sigma^-$  constants vs that for  $\sigma$  ( $r^2 = 0.94$  vs 0.90) indicates a possible resonance interaction between the substituent and this increased electron density at the benzylic position. This most probably implies that resonance effects dominate in a hyperconjugative interaction in the transition state. However, this improvement is largely due to the change in the substituent constant for the *p*-F group and may be an artifact of the substituents chosen.

Another important interpretation of these observations is to exclude a recent proposal for an alternative structure for an intermediate in this process. We<sup>16</sup> and others<sup>17</sup> have recently considered formation of a Re(V)-coordinated epoxide (eq 3),



where the rate-limiting step is migration of carbon not to rhenium but to the other diolate oxygen. Concerted fragmentation of this species might then generate the observed products by a path documented for earlier transition metals.<sup>18</sup> Were this to occur, it would involve migration of carbon *without* its electrons, in order to avoid hypervalent oxygen. We would therefore anticipate an improved correlation with  $\sigma^+$  ( $r^2$  actually drops to 0.84).<sup>19</sup> One would also expect inversion of stereochemistry (barring an unprecedented migration with retention) at one carbon relative to the second, and this is not observed. Thus we conclude that the second oxygen is not involved in the rate-limiting step.

**2. 1, 2-Diphenyl-1,2-diolates.** The obvious refinement of the initial experiment is to place an unsubstituted phenyl group on the second carbon. This provides the system a more finely balanced choice in the proposed alkyl migration. The required diols were prepared in a two-step procedure via Wittig reaction of benzylidene triphenylphosphorane with an appropriate aldehyde, followed by osmylation of the resulting stilbene.<sup>20</sup> The *anti,erythro*-diphenyldiolates were chosen (leading to *cis*-stilbene), although several were contaminated by small amounts of the two *threo* isomers. Rhenium diolates were prepared as before. All isomeric compounds were distinct in the <sup>1</sup>H NMR,

(14) (a) Allread, A. L. *J. Inorg. Nucl. Chem.* **1961**, *17*, 215–221. (b) Hinze, J.; Jaffé, H. H. *J. Am. Chem. Soc.* **1962**, *84*, 540–546. (c) Hinze, J.; Whitehead, M. A.; Jaffé, H. H. *J. Am. Chem. Soc.* **1963**, *85*, 148–154.

(15) Breslow, R. *Organic Reaction Mechanisms: An Introduction*, 2nd ed.; pp 88–90 Benjamin-Cummings: New York, 1969.

(16) Gable, K. P.; Juliette, J. J.; Gartman, M. A. *Organometallics* **1995**, *14*, 3138–3140.

(17) Espenson, J. H., personal communication.

(18) (a) Whinnery, L. L., Jr.; Henling, L. M.; Bercaw, J. E. *J. Am. Chem. Soc.* **1991**, *113*, 7575–7582. (b) Atagi, L. M.; Over, D. E.; McAlister, D. R.; Mayer, J. M. *J. Am. Chem. Soc.* **1991**, *113*, 870–874.

(19) Owen, J. R.; Saunders, W. H., Jr. *J. Am. Chem. Soc.* **1966**, *88*, 5809–5816.

(20) (a) Güsten, H.; Salzwedel, M. *Tetrahedron* **1967**, *23*, 187–191. (b) Kwong, H. L.; Sorato, C.; Ogino, Y.; Chen, H.; Sharpless, K. B. *Tetrahedron Lett.* **1990**, *31*, 2999–3000.

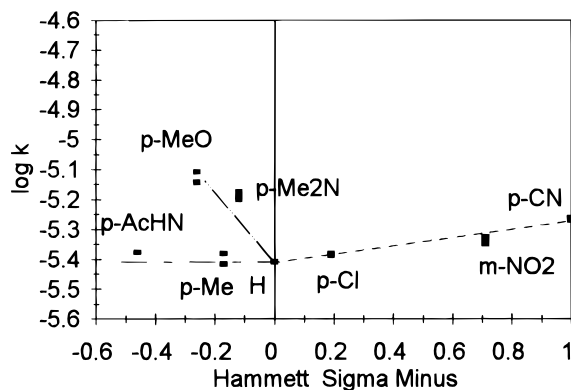


**Figure 2.** Hammett plot for extrusion of monosubstituted stilbenes. For the electron-withdrawing substituents vs  $\sigma^-$ ,  $\rho = 0.13$ ;  $r^2 = 0.94$ . Each rate is measured in triplicate.

and the first-order rates of fragmentation were followed by NMR at 50.9 °C.<sup>21</sup> The Hammett plot vs  $\sigma^-$  (values from ref 3b) is shown in Figure 2.

This plot shows several important features. First, there is clearly a curvature of this plot consistent with our expectation based on eq 1. The presence of the second phenyl ring offers a fine balance to the electronic effects in the substituted aryl ring, and the (nonlinear) shape of the curve offers important evidence that the overall symmetry of the diolate is broken on going to the transition state. This is the third independent piece of evidence against a concerted mechanism for this cycloreversion; such a hypothesis predicts a linear Hammett plot for both styrenes and stilbenes.<sup>22</sup>

The behavior (at least for electron-withdrawing groups) is also much better-correlated with  $\sigma^-$  than with  $\sigma$ . There are still significant elements of scatter on the electron-donating side; *p*-methyl and *p*-acetamido seem to be out of place compared to lone-pair-donating substituents *p*-methoxy and *p*-(dimethyl-amino). However, all are at least as fast as the unsubstituted case. The electron-withdrawing substituents are all roughly in correlation to one another. The lower  $\rho$  value reveals a moderated interaction between the aromatic ring and the reacting center in the transition state. Yet this second experiment raises significant questions. According to Scheme 1, we might expect that the electron-withdrawing region of the plot ( $\sigma^- > 0$ ) would show a slope similar to that seen in styrene extrusions; the slope is smaller (approximately 0.13 for stilbenes as opposed to approximately 0.42 for styrenes). Further, since reaction is apparently enhanced by electron-withdrawing groups, we expect a near-zero slope for  $\sigma^- < 0$ . We actually see much scatter and possibly a negative slope. The disturbing conclusion is that the electronic effects in stilbene extrusions have reversed from those seen in styrene extrusions! Finally, the overall rate behavior noted in Table 2 suggests additional fundamental differences in the behavior of styrene vs stilbene extrusion that are unexpected.

These apparent incongruities can be reconciled by noting the small size of these substituent effects ( $k(p\text{-MeO})/k(\text{H}) = 2$ ), and by close examination of the structures of the reactants. Resonance participation of the aromatic system requires proper orientation of the ring with the breaking bond in the transition state. We have performed molecular mechanics calculations on the phenylethanediolate and the 1,2-diphenylethanediolate and find the following (see Figure 3). With a single group,

(21) Although the two Hammett experiments were performed 10 °C apart, the low  $\Delta S^\ddagger$  observed (see Table 2) and the relatively small temperature difference allow comparison of the two.

(22) Huisgen, R. In *1,3-Dipolar Cycloaddition Chemistry*; Padwa, A., Ed.; Wiley: New York, 1984; Ch. 1.

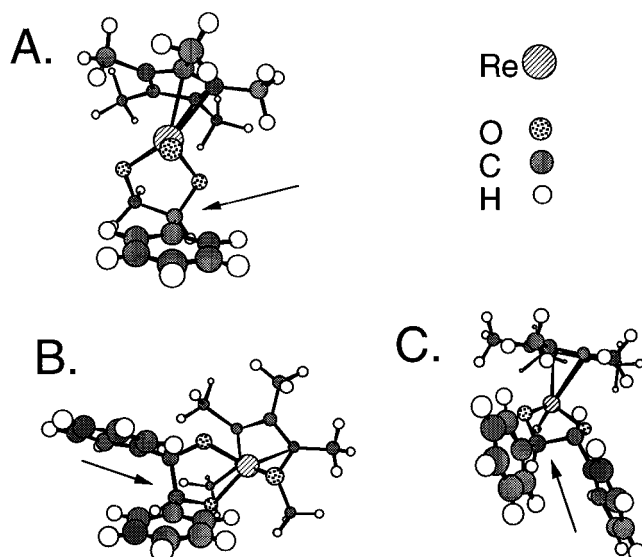


**Figure 3.** Predicted geometry of mono- and diphenyldiolates from molecular mechanics calculations using Spartans Sybyl force field. Arrows designate the carbon that is presumed to migrate predominantly. A: Phenylethanediolate (anti isomer). Note the absence of hindrance to rotation. B: *erythro*-1, 2-Diphenylethanediolate. Rotation of the phenyl groups creates severe Ph-Ph interactions. C: *threo*-1, 2-Diphenylethanediolate. This isomer has significantly more freedom of rotation about the Ph-C bonds.

there is essentially free rotation about the  $C_{\text{Ph}}\text{-C}$  bond; the ring can thus adopt any orientation necessary. However, when a second phenyl group is introduced, this freedom of rotation is severely limited. Projections down the Ph-C bond for minimized structures seen in Figure 3 show that the effect is to limit the ability of the ring to achieve maximal  $\pi$  overlap with the breaking C-O bond. (The more "axially" oriented C-O bond is chosen for reasons described below.) This fits well with the decreased  $\rho$  value.

Further experimental support is seen in comparison of activation parameters (Table 2) for several different diolates. Incorporation of the first phenyl group results in a significant acceleration of the cycloreversion by decreasing  $\Delta H^\ddagger$  by almost 2 kcal/mol. Placement of the second phenyl group in the *erythro* isomer (leading to *cis*-stilbene) not only fails to increase this effect, but actually causes a decreased effect. That the interaction of the phenyl groups is a controlling effect is seen in the  $\Delta H^\ddagger$  for *trans*-stilbene extrusion, which is now accelerated again. In Figure 3 one may see that rotation of the phenyl groups in this isomer does not result in the same steric interference that it does in the *erythro* isomer.

The acceleration due to lone-pair-containing groups is more puzzling. Two explanations are possible. First, given that twisting the rings will interfere with  $\pi$  interactions, we may be observing an inductive effect from these electronegative substituents. It seems surprising, though, that this would be larger than we see for such groups as *m*-NO<sub>2</sub> and *p*-CN. We failed to find a good correlation with multiparameter substituent effects<sup>3b</sup> that might support this hypothesis. A second alternative is that the substituted ring alters the diolate conformation so that the *unsubstituted* ring now has improved  $\pi$  interaction with its C-O bond. We do not see dramatic differences in the <sup>1</sup>H NMR spectral behavior for these compounds, but this reflects an averaged solution structure and may not be as informative as we desire.

In summary, these new data are once again more consistent with the intermediacy of a metallaoxetane than with alternative mechanistic proposals. They cannot be reconciled with an

“asynchronous” concerted mechanism and, combined with earlier results, reinforce the conclusion that this does not involve concerted cleavage of C–O bonds, or carbocation or free radical intermediates. A coordinated epoxide is also inconsistent with the accumulated evidence. Further, the stereospecificity and absence of significant solvent effects rule out a carbanionic intermediate. The curvature seen in the Hammett plots for extrusion of *cis*-stilbenes is in accord with the expectations of Scheme 1. Although the mechanism requires some rationalization concerning the conformation of phenyl rings and the degree of  $\pi$  interaction with the reaction center, molecular mechanics calculations are consistent with these assertions.

### Molecular Orbital Calculations: A Rationale for Changes in Bonding

Our experimental evidence has arrived at a general picture of the transition state for this process: cleavage of a single C–O bond such that the carbon atom picks up electron density. This picture is consistent with a migration of carbon from the more electronegative oxygen to the more electropositive rhenium and infers that the first-formed intermediate is a rhenaoxetane. Although rare, a few documented examples of this kind of reactivity have been reported.<sup>23,24</sup>

Such a rearrangement, carbon migrating with the bonding electron pair, is reminiscent of Wagner–Meerwein shifts in carbocation chemistry, pinacol rearrangements, and related processes.<sup>25</sup> These have two important requirements: availability of an empty orbital to which the carbon can migrate and the ability of the molecule to align the breaking bond with this orbital. We have used molecular orbital calculations at both the Extended Hückel (semiempirical) and Hartree–Fock (ab initio) levels to assess whether this is the case for these diolates. The results of these low-level calculations point to a predictive model for changes in bonding during C–O bond formation or fragmentation mediated by a metal.

Heavy atom geometries for all calculations were extracted from published X-ray crystal structures;<sup>26,27</sup> hydrogens were placed in calculated positions. In the case of Cp\*ReO<sub>3</sub>, the geometry of CpReO<sub>3</sub> was used, adding methyl groups to the ring in calculated geometries. Extended Hückel calculations were performed using parameters included in the program ICONCS (Quantum Chemistry Program Exchange). Hartree–Fock calculations were performed using a 3-21G(\*) basis set and substituting Tc for Re. This latter simplification is justified chemically by the similar behavior of Tc and Re compounds, although the thermodynamics of Tc oxo compounds have been shown to differ from those of the Re compounds.<sup>28</sup> Energies of the three highest occupied and three lowest unoccupied

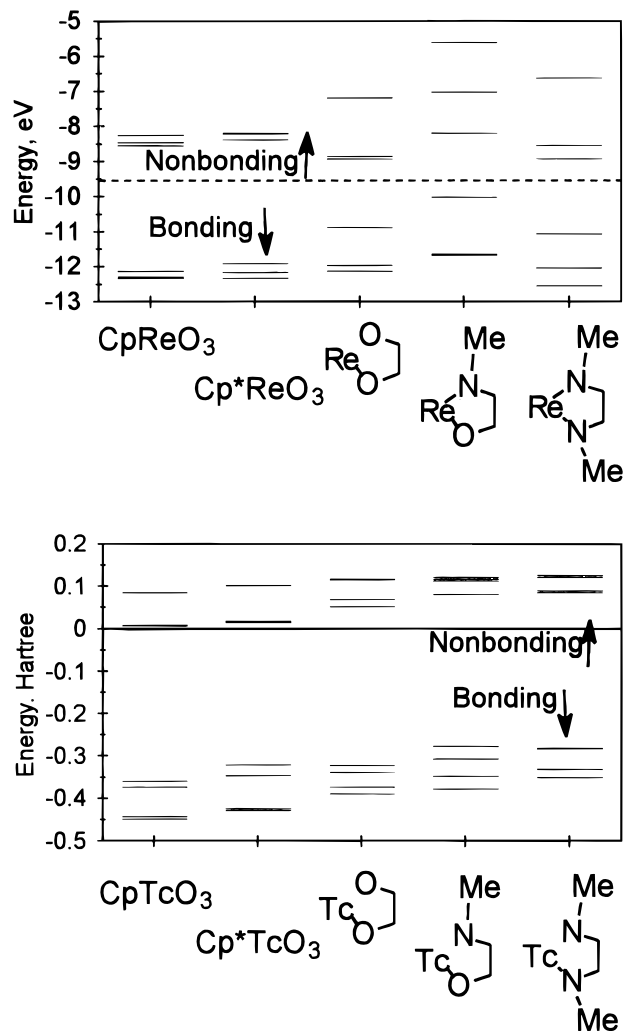


**Figure 4.** Top: frontier orbitals of rhenium compounds calculated by Extended Hückel methods. Bottom: frontier orbitals of technetium compounds calculated by HF methods using a 3-21G(\*) basis set.

orbitals described by these calculations are displayed in Figure 4; although the specific energies vary, the two approaches are in general agreement over the nature of the frontier orbitals for each compound and trends arising from structural variation at the metal.

In agreement with previous calculations,<sup>28</sup> we find from both methods that the HOMO of LMO<sub>3</sub> is a cyclopentadienyl-to-metal  $\pi$  orbital, though it has significant oxygen character as well. The LUMO is largely metal-centered, and M=O  $\pi^*$  in character (see Figure 5).<sup>29</sup> It is interesting to note that the primary effect of changing from Cp to Cp\* is seen in the increase in the HOMO energy; the LUMO is largely unaffected. This is undoubtedly due to the absence of metal-to-Cp  $\pi$  backbonding in these d<sup>0</sup> complexes. The orientation of the LUMO is such that a large lobe is directed toward the center of the MO<sub>3</sub> group. If an alkene interacts with either of these complexes in a Lewis acid/base fashion<sup>30</sup> (i.e., in the oxidation

(23) (a) van Asselt, A.; Burger, B. J.; Gibson, V. C.; Bercaw, J. E. *J. Am. Chem. Soc.* **1986**, *108*, 5347–5349. (b) Parkin, G.; Bunel, E.; Burger, B. J.; Trimmer, M. S.; van Asselt, A.; Bercaw, J. E. *J. Mol. Catal.* **1987**, *41*, 21–39. (c) Parkin, G.; van Asselt, A.; Leahy, D. J.; Whinnery, L.; Hua, N. G.; Quan, R. W.; Henling, L. M.; Schaefer, W. P.; Santarsiero, B. D.; Bercaw, J. E. *Inorg. Chem.* **1992**, *31*, 82–85. (d) Nelson, J. E.; Parkin, G.; Bercaw, J. E. *Organometallics* **1992**, *11*, 2181–2189. (e) Brown, S. N.; Mayer, J. M. *J. Am. Chem. Soc.* **1994**, *116*, 2219–2220.

(24) Tahmassebi, S. K.; Conroy, R. R.; Mayer, J. M. *J. Am. Chem. Soc.* **1993**, *115*, 7553–7554.

(25) It is, however, important to note the differences between this system and organic processes as has been done above. The absence of charge means that electronic effects will be dictated by changes in electronegativity. Thus, migration of carbon from (electronegative) oxygen to (electropositive) rhenium will result in the positive  $\rho$  seen here rather than the negative value seen in the organic processes cited.

(26) Kühn, F. E.; Herrmann, W. A.; Hahn, R.; Elison, M.; Blümel, J.; Herdtweck, E. *Organometallics* **1994**, *13*, 1601–1606.

(27) Herrmann, W. A.; Marz, D. W.; Herdtweck, E. *J. Organomet. Chem.* **1990**, *394*, 285–303.

(28) Pearlstein, R. M.; Davison, A. *Polyhedron* **1988**, *7*, 1981–1989.

(29) (a) Szyperki, T.; Schwerdtfeger, P. *Angew. Chem., Int. Ed. Engl.* **1989**, *28*, 1228–1230. (b) Wiest, R.; Leininger, T.; Jeung, G.-H.; Bénard, M. *J. Phys. Chem.* **1992**, *96*, 10800–10804.

(30) No symmetry restrictions were placed on the calculations, so the two highest HOMOs were not degenerate as expected from C<sub>s</sub> symmetry. However, the (HOMO-1) orbital was quite close in energy and quite similar in nature.

(31) De Meric de Bellefon, C.; Herrmann, W. A.; Kiprof, P.; Whitaker, C. R. *Organometallics* **1992**, *11*, 1072–1081.

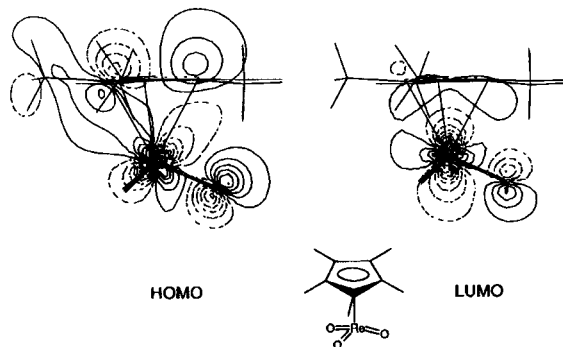


Figure 5. Frontier orbitals of  $\text{Cp}^*\text{ReO}_3$  from EHT calculations.

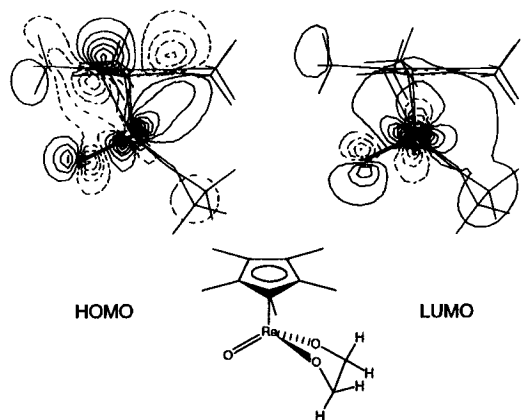


Figure 6. Frontier orbitals of  $\text{Cp}^*\text{Re}(\text{O})(\text{OCH}_2\text{CH}_2\text{O})$  from EHT calculations.

of strained alkenes<sup>32</sup>), the location of this orbital suggests that approach of the alkene trans to the Cp ring will be most favored.

In the diolate complex, the HOMO is again Cp–M  $\pi$  with significant metal lone pair character. One major difference between the two calculational approaches is that this orbital has more Cp–M  $\pi$  character in the EHT results, while the HF calculations give it more heteroatom lone pair character. (Compounds with N in place of O have a significantly higher heteroatom lone pair contribution.) The LUMO has the same general character as in the M(VII) trioxos, that is, mostly metal d, oriented to be antibonding with the lone terminal oxo ligand. A projection of this orbital (Figure 6) clearly shows that the two C–O bonds are placed in different orientations with respect to this orbital. One C–O bond (the “axially”-oriented one) aligns roughly with one lobe of this orbital, while the other lies roughly along the node. This offers an explanation for our earlier observation that a staggered geometry increased the rate of reaction; good orbital overlap of the breaking C–O bond with the LUMO promotes migration of carbon to rhenium. For N-substituted heterocycles, the ring has been shown to flatten;<sup>27</sup> our calculations show that in these cases both C–X bonds lie along the node of the LUMO (which again looks quite similar to that for the diolate; see Figure 7). A second generalization is that this orbital is higher in energy than that of the diolate, and that it has somewhat smaller metal orbital coefficients than in the diolate. Both of these effects are expected to raise the transition state energy for alkyl migration and are thus consistent with the reported reluctance of these compounds to extrude alkene.<sup>27</sup>

From these results, a general scheme for bonding changes during this reaction can be developed (Scheme 2). In diolate cycloreversion, the rate-limiting step is the initial migration of

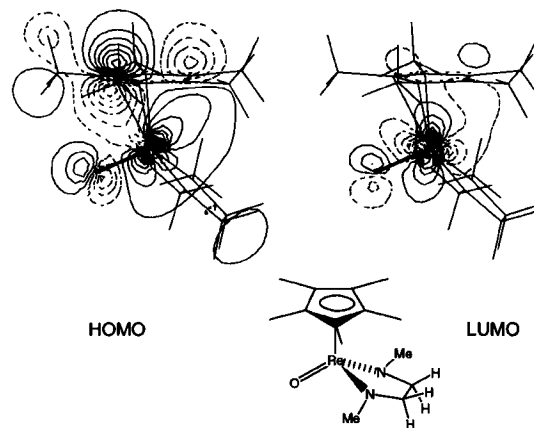
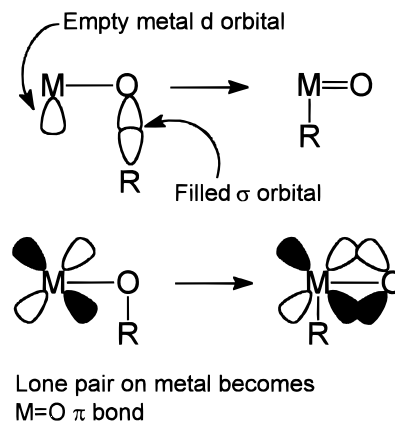


Figure 7. Frontier orbitals of  $\text{Cp}^*\text{Re}(\text{O})(\text{MeNCH}_2\text{CH}_2\text{NMe})$  from EHT calculations.

### Scheme 2



carbon to rhenium. This requires interaction of the filled C–O orbital with the (empty) LUMO at rhenium. Concurrently, the lone pair at the metal center is delocalized by interaction with the oxygen orbital from which the carbon migrates, resulting in a new M=O  $\pi$  bond. Collapse of the metallaoxetane intermediate to the observed products is formally analogous to formation and cleavage of metallacyclobutanes and likely involves slippage of the metallacycle to a coordinated alkene, followed by loss of the alkene.

Viewing oxidations (either of strained alkenes by  $\text{Cp}^*\text{ReO}_3$ <sup>32</sup> or of alkenes in general by other metal oxo complexes) as the microscopic reverse of this process, one can see that formation of the metallacycle is again analogous to other [2 + 2] chemistry of M=X complexes.<sup>33</sup> The new element is now migration of a metal alkyl to a terminal oxo ligand. (This is topologically similar to known migrations to metal carbenes.<sup>34</sup>) Turning around the logical elements described above, this migration must

(33) This is a well-documented process, particularly for early metal oxo compounds. See: (a) deWith, J.; Horton, A. D.; Orpen, A. G. *Organometallics* **1993**, *12*, 1493–1496. (b) Klein, D. P.; Hayes, J. C.; Bergman, R. G. *J. Am. Chem. Soc.* **1988**, *110*, 3704–3706. (c) Klein, D. P.; Bergman, R. G. *J. Am. Chem. Soc.* **1989**, *111*, 3079–3080. (d) Hartwig, J. F.; Bergman, R. G.; Anderson, R. A. *J. Am. Chem. Soc.* **1990**, *112*, 3234–3236. (e) Carney, M. J.; Walsh, P. J.; Hollander, F. J.; Bergman, R. G. *J. Am. Chem. Soc.* **1990**, *112*, 6426–6428. (f) Vaughan, G. A.; Sofield, C. D.; Hillhouse, G. L.; Rheingold, A. L. *J. Am. Chem. Soc.* **1989**, *111*, 5491–5493. (g) Walsh, P. J.; Baranger, A. M.; Bergman, R. G. *J. Am. Chem. Soc.* **1992**, *114*, 1708–1719. (h) Baranger, A. M.; Walsh, P. J.; Bergman, R. G. *J. Am. Chem. Soc.* **1993**, *115*, 2753–2763.

(34) (a) Hayes, J. C.; Pearson, G. D. N.; Cooper, N. J. *J. Am. Chem. Soc.* **1981**, *103*, 4648–4650. (b) Jernakoff, P.; Cooper, N. J. *Organometallics* **1986**, *5*, 747–751. (c) Winter, M. J. *Polyhedron* **1989**, *8*, 1583–1588. (d) Winter, M. J.; Woodward, S. *J. Chem. Soc., Chem. Commun.* **1989**, 457–458.

(32) Gable, K. P.; Phan, T. N. *J. Am. Chem. Soc.* **1993**, *115*, 3036–3037.

occur with carbon maintaining formal possession of the electrons in the M–C bond. This is a consequence of microscopic reversibility. Therefore, the M–C bond must interact (in the transition state) with an *empty orbital on oxygen*. The available empty orbital is the  $\pi^*$  component of the M=O bond. Perturbation MO theory suggests that to optimize this interaction one should maximize spatial overlap and minimize the energy difference between the two orbitals. In most cases, the geometry of the M(R)O<sub>n</sub> fragment will fix spatial overlap. The primary determinant of whether this mechanism is viable in any specific circumstance, then, is the energetic difference between the level of the C–M bonding orbital and the M=O  $\pi^*$  orbital. The structurally variable component of this interaction is going to be the energy of the M=O antibonding orbital. The same computational observations have been made previously for alkyl migration to M=CH<sub>2</sub>,<sup>35</sup> and a very similar argument has recently been advanced by Brown and Mayer to explain related alkyl-to-oxo migrations.<sup>36</sup>

This offers us both a predictive model for where one might see such a process and a rationale for why it may be limited to certain specific kinds of systems.<sup>37</sup> Metal alkyl-oxo complexes may be generally stable<sup>38</sup> to alkyl migration if there are only one or two oxo ligands, provided that orientation of the M=O  $\pi$  bond precludes the necessary transition state overlap. (Alternatively, the strong M=O bonds found in earlier transition metal systems may thermodynamically disfavor migration.) Further, the lack of competition for  $\pi$  acceptor orbitals on the metal results in strong  $\pi$  interaction, high bond order and thus a high-lying antibonding orbital.

For compounds with multiple oxo ligands the situation is fundamentally different, particularly for late third-row transition metals. Competition for acceptor orbitals on the metal by multiple oxo ligands will weaken the average  $\pi$  bond (and decrease the bond order) with a consequent decrease in the  $\pi^*$  orbital energy (the so-called “spectator oxo” effect).<sup>39</sup> Further, an appropriate donor ligand (e.g., cyclopentadienyl) will compound this effect. (Recall that one of the unusual features of osmylation chemistry is the dramatic *increase* in reaction rate induced by Lewis basic amine donor ligands.)<sup>40</sup> On the other hand, simply weakening the M=O interaction by going to first- or second-row metals may open alternative mechanisms (particularly electron transfer). Cycloadditions/cycloreversions add a significant additional factor in that geometrical restrictions may inherently limit alternative processes (e.g., C–H activation) or provide an entropic boost to the reaction.

(35) (a) Carter, E. A.; Goddard, W. A. *J. Am. Chem. Soc.* **1987**, *109*, 579–580. (b) Carter, E. A.; Goddard, W. A. *Organometallics* **1988**, *7*, 675–686.

(36) (a) Brown, S. N. Ph. D. Thesis, University of Washington **1995**. (b) Mayer, J. M., personal communication.

(37) (a) Reichle, W. T.; Carrick, W. L. *J. Organomet. Chem.* **1970**, *24*, 419–426. (b) Nugent, W. A.; Harlow, R. L. *J. Am. Chem. Soc.* **1980**, *102*, 1759–1760. (c) Brown, S. N.; DuMez, D. D.; Mayer, J. M. *Abstracts of the 207th National Meeting of the American Chemical Society*, San Diego, CA. American Chemical Society: Washington; 1994. INOR 168. (d) See also refs 23 and 24.

(38) Several examples: (a) Herrmann, W. A.; Eder, S. J.; Scherer, W. *J. Organomet. Chem.* **1993**, *454*, 257–261 (b), Herrmann, W. A.; Serrano, R.; Küsthardt, U.; Ziegler, M. L.; Guggolz, E.; Zahn, T. *Angew. Chem., Int. Ed. Engl.* **1984**, *23*, 515–517. (c) Legzdins, P.; Rettig, S. J.; Sanchez, L. *Organometallics* **1985**, *4*, 1470–1471. (d) Schrauzer, G. N.; Hughes, L. A.; Strampach, N.; Ross, F.; Ross, D.; Schlemper, E. O. *Organometallics* **1983**, *2*, 481–485.

(39) Rappé, A. J.; Goddard, W. A. III *J. Am. Chem. Soc.* **1982**, *104*, 448–456.

(40) Criegee, R.; Marchand, B.; Wannowius, H. *Justus Liebigs Ann. Chem.* **1942**, *550*, 99–133.

**Table 3.** First-Order Rate Constants for the Extrusion of Substituted Styrenes at 40.1 °C

substituent	$k_{\text{obs}}$ , $10^{-6} \text{ s}^{-1}$	substituent	$k_{\text{obs}}$ , $10^{-6} \text{ s}^{-1}$
4-MeO	5.07	4-Me	5.74
	5.54		6.32
	5.12		6.27
4-F	5.57	4-Cl	9.40
	5.81		8.30
	5.66		9.62
4-CF <sub>3</sub>	11.6	3-NO <sub>2</sub>	12.6
	12.9		14.2
H <sup>a</sup>			13.4

<sup>a</sup> Obtained from Eyring plot; see ref 2: 6.6.

**Table 4.** First-Order Rate Constants for the Extrusion of Substituted *cis*-Stilbenes at 50.1 °C

substituent	$k_{\text{obs}}$ , $10^{-6} \text{ s}^{-1}$	substituent	$k_{\text{obs}}$ , $10^{-6} \text{ s}^{-1}$
4-AcNH	4.16	4-Me <sub>2</sub> N	6.71
	3.78		6.34
	3.56		6.40
4-MeO	7.24	4-Me	3.85
	7.76		3.82
	7.58		4.16
4-Cl	3.92	4-CN	5.36
	3.68		5.46
3-NO <sub>2</sub>	4.72		5.49
	4.62		
	4.49		
H <sup>a</sup>			

<sup>a</sup> H Obtained from Eyring Plot; see below: 3.91.

**Table 5.** Kinetic Data and Eyring Parameters for the extrusion of *cis*-Stilbene<sup>a</sup>

temp (°C)	$k_{\text{obs}}$ , $10^{-5} \text{ s}^{-1}$
85	28.0
75.4	8.78
60.9	1.51
50.9	0.391
40.9	0.0989

<sup>a</sup> From a plot of  $\ln(k/T)$  vs  $1/T$ , slope = 14047.01, intercept = 25.14  $r^2 = 0.9999$ .  $\Delta H^\ddagger$ , = 27.9 ± 0.2 kcal/mol.  $\Delta S^\ddagger$  = 2.73 ± 0.81 cal/(mol·K).

## Conclusion

Hammett studies on cycloreversion of phenylethanediolates confirms that cleavage of the C–O bond occurs with buildup of electron density on the reacting carbon. Further, evidence for the importance of a  $\pi$  interaction between the phenyl substituent and the breaking C–O bond is seen. These observations are consistent with rate-determining alkyl migration to form a rhenaoxetane. Molecular orbital calculations are consistent with this assertion, and offer a predictive explanation of the bonding changes occurring in this system.

## Experimental Section

General methods for preparation of the diolates and for execution of kinetic experiments have been described previously.<sup>2,6</sup> All diols were obtained from osmylation of the corresponding alkene.<sup>20</sup> All NMR measurements were conducted in C<sub>6</sub>D<sub>6</sub> and referenced to residual solvent protons at 7.15 ppm or to solvent carbons at 128 ppm. Yields were not optimized given the need for maximum purity. Kinetic rate constants are reported in Tables 3–6; unless otherwise noted, disappearance of the anti isomer was followed.

**Synthesis of (Pentamethylcyclopentadienyl) Oxorhenium 1-Arylethane-1,2-diolate Complexes.** The syntheses were all accomplished in the same manner. A representative preparation is described here; yields and characterization for other compounds are below. A round-bottom flask was charged with Cp\*ReO<sub>3</sub> (70.6 mg, 0.191 mmol), 1-(3-

**Table 6.** Kinetic Data and Eyring Parameters for the Extrusion of *trans*-Stilbene<sup>a</sup>

temp (°C)	k <sub>obs</sub> , 10 <sup>-5</sup> s <sup>-1</sup>
55.0	33.7
50.1	21.7
40.2	6.02
30.2	1.56
20.6	0.426

<sup>a</sup> From a plot of  $\ln(k/T)$  vs  $1/T$ , slope = 12134.94, intercept = 23.25  $r^2 = 0.9992$ .  $\Delta H^\ddagger = 24.1 \pm 0.7$  kcal/mol.  $\Delta S^\ddagger = -1.01 \pm 0.81$  cal/(mol·K).

nitrophenyl)ethane-1,2-diol (0.10 g, 123 mmol), polymer-bound triphenylphosphine (76 mg, 1.2 equiv), *p*-toluenesulfonic acid (36 mg, 78 mmol), and molecular sieves (0.5 g). The flask was affixed to a double-ended frit and evacuated for 15 min. THF (15 mL) was added and the mixture stirred at room temperature overnight. The purple mixture was filtered and the filtrate reduced to a solid. The residue was chromatographed on silica using CHCl<sub>3</sub> to elute any remaining Cp\*ReO<sub>3</sub> and diol. The diolate was eluted with acetone. Removal of the solvent followed by recrystallization from hexanes or pentane afforded the diolate as a purple-red solid (20 mg, 0.038 mmol, 20% based on rhenium).

**(Pentamethylcyclopentadienyl) oxorhenium (3-nitrophenyl)ethane-1,2-diolate:** 2:1 mixture of isomers. <sup>1</sup>H NMR: major (anti) isomer: 8.33 (m, 1H), 7.76–7.70 (m, 1H), 6.88–6.70 (m, 1H) (other aromatic signal obscured by solvent), 5.03 (dd,  $J = 5.5$  Hz, 10.5 Hz, 1H), 4.10 (dd,  $J = 5.6$  Hz, 10.0 Hz, 1H), 3.09 (t,  $J = 10.5$  Hz, 1H), 1.66 (s, 15H). Minor (syn) isomer: 8.14 (m, 1H), 7.5 (m, 1H), (other aromatic signals obscured by solvent), 4.25 (t,  $J = 7.0$  Hz, 1H), 3.87 (d,  $J = 7.6$  Hz), 1.65 (s, 15H). <sup>13</sup>C NMR: 144.3, 143.6, 133.1, 132.7, 122.5, 122.2, 122.0, 121.8, 119.3, 108.4, 108.3, 92.0, 91.2, 87.6, 87.2, 11.1, 11.0. Additional aromatic peaks obscured by solvent. Anal. for C<sub>18</sub>H<sub>22</sub>NO<sub>3</sub>Re: Calc (Found): C 41.69 (41.52), H 4.28 (4.24), N 2.70 (2.62).

**(Pentamethylcyclopentadienyl) oxorhenium [4-(trifluoromethyl)phenyl]ethane-1,2-diolate:** 15% yield of a 3.5:3 ratio of isomers. <sup>1</sup>H-NMR: Major (anti) isomer: 7.40–7.17 (m, overlap with minor isomer), 5.12 (dd,  $J = 5.7$ , 10.9 Hz, 1H), 4.17 (dd,  $J = 5.7$ , 10.0 Hz, 1H), 3.16 (t,  $J = 10.7$  Hz, 1H), 1.68 (s, 15H). Minor (syn) isomer: Aromatic signals overlap major isomer. 4.36 (dd,  $J = 6.7$ , 6.3 Hz, 1H), 3.99–3.95 (m, 2H), 1.67 (s, 15H). <sup>13</sup>C-NMR: 144.1, 130.3, 126.4, 108.1, 108.0, 92.1, 91.5, 86.9, 86.9, 10.8, 10.8. Remainder of aromatic signals obscured by solvent. Anal. for C<sub>19</sub>H<sub>22</sub>F<sub>3</sub>O<sub>3</sub>Re: Calc (Found) C 42.14 (42.16), H 4.09 (4.12).

**(Pentamethylcyclopentadienyl) oxorhenium (4-chlorophenyl)ethane-1,2-diolate:** deep purple solid as a 1:1 mixture of isomers in 30% yield. <sup>1</sup>H-NMR: Anti isomer: 7.18–7.06 (m, overlap with syn isomer), 5.13 (dd,  $J = 5.9$  Hz, 10.7 Hz, 1H), 4.17 (dd,  $J = 5.6$  Hz, 9.9 Hz, 1H), 3.22 (t,  $J = 10.5$  Hz, 1H), 1.66 (s, 15H). Syn isomer: 7.18–7.06 (m, overlap with anti isomer), 4.33 (t,  $J = 7.5$  Hz, 1H), 3.99 (d,  $J = 7.5$  Hz, 2H), 1.66 (s, 15H). <sup>13</sup>C-NMR: 128.7, 128.9, 108.1, 108.1, 92.4, 92.0, 87.3, 87.2, 11.1, 11.1. Remainder of aromatic signals obscured by solvent. Analysis for C<sub>18</sub>H<sub>22</sub>ClO<sub>3</sub>Re: Calc (Found) C 42.56 (42.44), H 4.36 (4.31).

**(Pentamethylcyclopentadienyl) oxorhenium (4-fluorophenyl)ethane-1,2-diolate:** purple solid as a 1:1 mixture of isomers in 10% yield. <sup>1</sup>H-NMR: Anti isomer: 7.2–7.1 (m, 2H), 6.89–6.78 (tt,  $J = 7.5$ , 8.7 Hz, 2H), 5.15 (dd,  $J = 5.1$  Hz, 10.6 Hz, 1H), 4.20 (dd,  $J = 5.8$  Hz, 10.2 Hz, 1H), 3.27 (t,  $J = 10.5$  Hz, 1H), 1.67 (s, 15H). Syn isomer: 7.2–7.1 (m, 4H), 4.35 (t,  $J = 7.5$  Hz, 1H), 4.01 (d,  $J = 7.5$  Hz, 2H), 1.681. <sup>13</sup>C-NMR: 163.8, 161.5, 129.1 (d,  $J = 6$  Hz), 128.9 (d,  $J = 7.6$  Hz), 115.1 (d,  $J = 6$  Hz), 114.9 (d,  $J = 6$  Hz), 108.0, 92.5, 92.0, 87.3, 87.2, 11.1, 11.1. Additional aromatic peaks obscured by solvent. Anal. for C<sub>18</sub>H<sub>22</sub>FO<sub>3</sub>Re: Calc (Found) C 43.98 (50.61), 4.51 (4.56).

**(Pentamethylcyclopentadienyl) oxorhenium (4-methylphenyl)ethane-1,2-diolate:** purple solid as a 1:1 mixture of isomers in 10% yield. <sup>1</sup>H-NMR: Anti isomer: 7.41 (d,  $J = 7.9$  Hz, 2H), 7.29 (d,  $J = 7.9$  Hz, 2H), 5.32 (dd,  $J = 5.6$ , 10.5 Hz, 1H), 4.32 (dd,  $J = 5.65$ , 10.1 Hz, 1H), 3.43 (t,  $J = 10.5$  Hz, 1H), 2.16 (s, 3H), 1.69 (s, 15H). Syn

isomer: 7.07–6.99 (m, 4H), 4.52 (dd,  $J = 6.0$ , 9.0 Hz, 1H), 4.23–4.10 (m, 2H), 2.11 (s, 3H), 1.702 (s, 15H). <sup>13</sup>C-NMR: 139.3, 138.5, 136.8, 136.6, 129.3, 129.1, 129.1, 129.0, 108.0, 107.9, 93.2, 92.9, 87.3, 11.1, 11.1. Anal. for C<sub>19</sub>H<sub>25</sub>O<sub>3</sub>Re: Calc (Found) C 46.80 (46.72), H 5.17 (5.28).

**(Pentamethylcyclopentadienyl) oxorhenium (4-methoxyphenyl)ethane-1,2-diolate:** purple solid as a 52:48 mixture of isomers in 10% yield. <sup>1</sup>H-NMR: Major (anti) isomer: 7.39 (d,  $J = 8.7$  Hz, 2H), 7.25 (d,  $J = 8.6$  Hz, 2H), 5.25 (dd,  $J = 5.6$ , 10.6 Hz, 1H), 4.27 (dd,  $J = 5.56$ , 10.1 Hz, 1H), 3.39 (t,  $J = 10.3$  Hz, 1H), 3.32 (s, 3H), 1.71 (s, 15H). Minor (syn) isomer: 6.84–6.72 (m, 4H), 4.47 (dd,  $J = 6.1$ , 8.8 Hz, 1H), 4.18–4.09 (m, 2H), 3.27 (s, 3H), 1.71 (s, 15H). <sup>13</sup>C-NMR: 130.3, 129.8, 114.0, 113.9, 108.0, 108.0, 92.8, 92.5, 86.8, 86.7, 54.7, 11.2, 11.1. Remaining signals obscured by solvent. Anal. for C<sub>19</sub>H<sub>25</sub>O<sub>4</sub>Re: Calc (Found) C 45.31 (45.26), H 5.00 (5.03).

**(Pentamethylcyclopentadienyl) oxorhenium *cis*-1,2-diphenylethanediolate:** A representative preparation for the stilbene diolates is given. A round-bottom flask was charged with Cp\*ReO<sub>3</sub> (109 mg, 0.29 mmol), polymer-bound PPh<sub>3</sub> (160 mg, 1.2 equiv), *meso*-hydrobenzoin (190 mg, 0.87 mmol), TsOH (60 mg, 0.32 mmol), and ground molecular sieves (Linde 4A, 0.5 g). The flask was affixed to a double-ended frit and evacuated, and then dry THF (10 mL) was condensed into the flask under vacuum and the reaction mixture stirred at room temperature overnight. The purple mixture was filtered and the THF removed in vacuo. Hexanes (15 mL) were condensed into the flask, and the residual *meso*-hydrobenzoin was crystallized out. The diolate was isolated as a purple solid in 20% yield (30 mg, 0.19 mmol). <sup>1</sup>H-NMR (C<sub>6</sub>D<sub>6</sub>): 7.34 (dd,  $J = 9$ , 1.4 Hz, 4H), 6.99 (t,  $J = 7.4$  Hz, 4H), 6.88–6.83 (m, 2H), 4.93 (s, 2H), 1.72 (s, 15H). <sup>13</sup>C-NMR (C<sub>6</sub>D<sub>6</sub>): 141.8, 128.8, 126.9, 108.1, 94.8, 11.2. Additional aromatic peaks obscured by solvent. Anal. for C<sub>24</sub>H<sub>27</sub>O<sub>3</sub>Re: Calc (Found) C 52.44 (52.26), H 4.95 (4.93).

**(Pentamethylcyclopentadienyl) oxorhenium *trans*-1,2-diphenylethanediolate:** 10% yield. <sup>1</sup>H-NMR: 7.2–6.9 (m, 10H), 5.24 (d,  $J = 9.7$  Hz, 1H), 4.50 (d,  $J = 9.6$  Hz, 1H), 1.73 (s, 15H). <sup>13</sup>C-NMR: 141.6, 141.2, 137.8, 129.1, 128.9, 126.9, 108.3, 100.4, 99.7, 11.2. Additional aromatic peaks obscured by solvent. Anal. for C<sub>24</sub>H<sub>27</sub>O<sub>3</sub>Re: Calc (Found) C 52.44 (52.21), H 4.95 (4.94).

**(Pentamethylcyclopentadienyl) oxorhenium 1-(4-acetamidophenyl)-2-phenylethanediolate:** 15% yield. <sup>1</sup>H-NMR (C<sub>6</sub>D<sub>6</sub>): 7.64–7.61 (m, 2H), 7.35 (d,  $J = 7.4$  Hz, 2H), 7.29 (m, 2H), 7.09–7.0 (m, 2H), 6.96–6.86 (m, 2H), 4.95 (s, 2H), 1.72 (s, 15H), 1.3 (s, 3H). <sup>13</sup>C-NMR: 167.5, 141.9, 130.8, 129.0, 128.7, 126.0, 118.7, 108.2, 94.4, 94.5, 30.2, 11.2. Other peaks obscured by solvent. Anal. for C<sub>26</sub>H<sub>30</sub>NO<sub>3</sub>Re: Calc (Found) C 52.86 (50.58), H 5.12 (4.81), N 2.37 (2.32).

**(Pentamethylcyclopentadienyl) oxorhenium 1-[4-(dimethylamino)phenyl]-2-phenylethanediolate:** 10% yield. <sup>1</sup>H-NMR: 7.48 (d,  $J = 7.3$  Hz, 2H), 7.34 (d,  $J = 8.8$ , 2H), 7.15–7.0 (m, 3H), 6.52–6.43 (m, 2H), 5.02 (d,  $J = 6.7$  Hz, 1H), 4.92 (d,  $J = 6.7$  Hz, 1H), 2.32 (s, 6H), 1.75 (s, 15H). <sup>13</sup>C-NMR: 149.8, 142.3, 129.8, 129.3, 112.1, 107.9, 94.6, 40.1, 11.2. Additional peaks obscured by solvent. Anal. for C<sub>26</sub>H<sub>32</sub>NO<sub>3</sub>Re: Calc (Found) C 52.68 (52.65), H 5.44 (5.21), N 2.36 (2.35).

**(Pentamethylcyclopentadienyl) oxorhenium 1-(4-methoxyphenyl)-2-phenylethanediolate:** 10% yield. <sup>1</sup>H-NMR: 7.45–7.2 (m, 5H), 6.7–6.5 (m, 4H), 4.93 (dd,  $J = 6.7$  Hz, 2H), 1.74 (s, 15H). <sup>13</sup>C-NMR: 164.2, 141.8, 108.3, 94.4, 93.7, 54.6, 11.2. Additional peaks obscured by solvent. Anal. for C<sub>25</sub>H<sub>29</sub>O<sub>4</sub>Re: Calc (Found) C 51.80 (51.74), H 5.04 (5.16).

**(Pentamethylcyclopentadienyl) oxorhenium 1-(4-methylphenyl)-2-phenylethanediolate:** 10% yield. <sup>1</sup>H NMR: 7.45–7.2 (m, 5H), 6.7–6.5 (m, 4H), 4.93 (dd,  $J = 6.7$  Hz, 2H), 1.74 (s, 15H). <sup>13</sup>C NMR: 142.0, 138.9, 136.1, 129.6, 108.0, 94.8, 94.7, 20.9, 11.2. Additional peaks obscured by solvent. Anal. for C<sub>25</sub>H<sub>29</sub>O<sub>3</sub>Re: Calc (Found) C 53.27 (53.31), H 5.19 (5.26).

**(Pentamethylcyclopentadienyl) oxorhenium 1-(4-chlorophenyl)-2-phenylethanediolate:** 20% yield. <sup>1</sup>H NMR: 7.26 (d,  $J = 7.1$  Hz, 2H), 7.1–7.08 (m, 2H), 7.03–6.9 (m, 5H), 4.78 (dd,  $J = 6$  Hz, 2H), 1.74 (s, 15H). <sup>13</sup>C NMR: 141.4, 139.3, 133.5, 132.7, 132.3, 129.7, 127.4, 127.1, 108.3, 94.9, 93.8, 11.1. Anal. for C<sub>24</sub>H<sub>24</sub>ClO<sub>3</sub>Re: Calc (Found) C 49.35 (49.21), H 4.49 (4.53).



**(Pentamethylcyclopentadienyl) oxorhenium 1-(4-cyanophenyl)-2-phenylethanediolate:** 10% yield.  $^1\text{H}$  NMR: 7.4–7.1 (m, 9H), 4.77 (dd,  $J = 6.8\text{Hz}$ , 2H), 1.69.  $^{13}\text{C}$  NMR: 171.9, 133.7, 131.9, 131.2, 130.4, 130.3, 117.2, 108.6, 94.9, 93.3, 11.1. Additional peaks obscured by solvent.

**(Pentamethylcyclopentadienyl) oxorhenium 1-(3-nitrophenyl)-2-phenylethanediolate:** 10% yield.  $^1\text{H}$ -NMR ( $\text{C}_6\text{D}_6$ ): 8.15 (m, 1H), 7.6 (m, 1H), 7.5 (dd,  $J = 7.7\text{ Hz}$ , 1H), 7.1–6.8 (m, 6H), 4.78 (dd,  $J = 7.24, 1.2\text{ Hz}$ ), 1.70 (s, 15H),  $^{13}\text{C}$ -NMR: 143.9, 141.1, 133.6, 132.4, 131.6, 128.5, 127.3, 123.1, 121.7, 108.5, 95.5, 93.2, 11.1. Additional peak obscured by solvent.

**Calculations.** Molecular mechanics calculations were performed using the Sybyl force field in the program Spartan (Wavefunction, Inc., Irvine, CA) operating on a Silicon Graphics IRIS-Indigo workstation. The coordination geometry of rhenium ( $\eta\text{-C}_5\text{ReO}_3$ ) was fixed at that seen in the solid state structure of the ethanediolate.<sup>27</sup> Phenyl groups were placed on the diolate ring and minimized to a gradient of  $<10$  cal/mol. The phenyl ring was then rotated to an O–C–C–C dihedral

angle of approximately  $90^\circ$  and re-minimized to evaluate whether a conformer with optimal  $\pi$  interaction with the breaking C–O bond was present. Finally, a conformational search was executed by varying all C–Ph dihedrals. No correction was made for Re–C nonbonded interactions.

Molecular orbital calculations at the Hartree–Fock level were executed on the same system, using the appropriate Spartan module. Published X-ray crystal structure data was used for heavy-atom geometries; hydrogens were placed in calculated positions by Spartan. No geometry optimization was performed. Technetium was used as the core element in place of rhenium.

Extended Hückel calculations were performed using the program ICONCS (Quantum Chemistry Program Exchange, University of Indiana, Bloomington, IN) operating on a PC. Geometries were the same used for ab initio calculations.

JA952537W